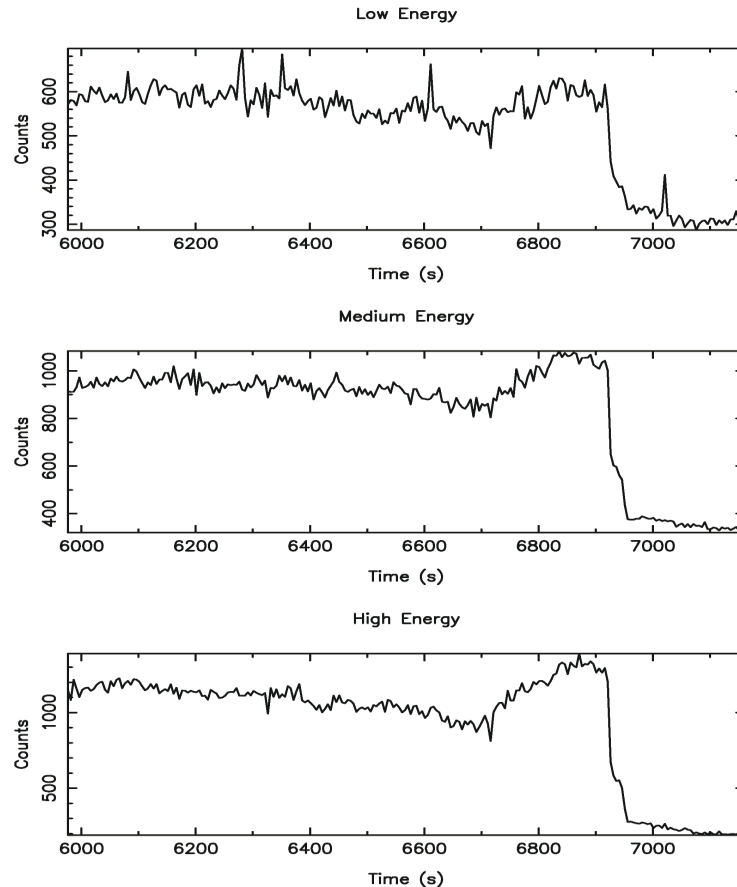


Division of ESA, at ESTEC. In particular J. Verveer and S. Andersson who provided engineering support during the instrument development and at the telescope, and P. Verhoeve and T. Peacock for the optimisation of the detector performance and its detailed evaluation. The astronomical observations performed with S-Cam and the data interpretation have been carried out by F. Favata and M. A. C. Perryman, supported by A. Reynolds.

□

Peter Moore (pcm@ing.iac.es)

Figure 1. Eclipse transition of the binary UZ For in three energy bands (low, medium and upper). The low energy band extends from 1800 nm to 620 nm; the medium energy band extends from 620 nm to 525 nm and the high energy band from 525 nm to 215 nm. The counts were provided by all the 36 elements of the array, without any filtering procedure.



## INTEGRAL: A Simple and Friendly Integral Field Unit Available at the WHT

Begoña García-Lorenzo<sup>1</sup>, Santiago Arribas<sup>2</sup> and Evencio Mediavilla<sup>2</sup>

<sup>1</sup>: Isaac Newton Group of Telescopes (ING); <sup>2</sup>: Instituto de Astrofísica de Canarias

Integral-field spectroscopy (IFS) has merited much attention in recent years due to its advantages with respect to classical *sequential* 2-D spectroscopic techniques (e.g., long-slit scans, Fabry-Perot) when studying relatively small extended objects. IFS is able to *simultaneously* obtain a spectrum for each spatial sample of a two-dimensional field.

Most of the advantages of the IFS technique are direct consequences of the simultaneity when recording spatial and spectral information. Indeed, there is no need to worry about the differential atmospheric refraction, nor to adapt the slit width (spectral resolution) to the seeing conditions. The configuration of IFS makes unnecessary an accurate

centering of the slit. The simultaneity does not only imply a more efficient way to observe but, more importantly, it guarantees a great homogeneity in the data. Several implementations of the IFS technique have been developed, based in the use of fibres, microlenses, micro-mirrors, or mixed solutions.

Early implementations of fibre projects at the Roque de los Muchachos Observatory were led by Peter Gray more than a decade ago. During all this time, the WHT has played an important role in the development of the IFS. Several fibre IFS instruments have been built (HEXAFLEX, Arribas et al., 1991; 2D-FIS, García et al., 1994, and now INTEGRAL, Arribas et al., 1998a). More recently SAURON (de Zeeuw et al., 2000), which is

based on the microlenses approach has also been successfully used at the WHT. Future projects include TEIFU and OASIS, which combine the advantages of IFS and AO.

### INTEGRAL

INTEGRAL is used in combination with the WYFFOS spectrograph (Bingham et al., 1994), and it is mounted in the Nasmyth 1 platform (GHRIL) of the WHT (see Figure 1).

In the standard configuration three fibre bundles (see Figure 2 for their main characteristics) are simultaneously connected at the entrance *pseudoslit* of the WYFFOS spectrograph. The bundles can be

easily interchanged at the focal plane, with an overhead of a few seconds. Hence, depending on the prevailing seeing conditions and/or spatial requirements, the instrument can be easily optimised for the scientific program. The bundles can also be oriented to the desired sky position angle.

For any particular grating the spectral resolution depends on the fibre bundle. This is a direct consequence of the different sizes of the fibres. Table 1 lists the mean spectral resolution and linear dispersions for different gratings and bundles.

Due to the fact that the fibre bundles are directly connected to the focal plane without the need of pre-optics (optical derotator, focal enlarger/reducer, etc), INTEGRAL + WYFFOS is relatively efficient (1 count/s/Å for a 15 mag object at  $\lambda = 5000 \text{ \AA}$ ). The focal ratio degradation (FRD) produced by the fibres is used to convert the  $f/11$  input from the telescope to the  $f/8$  of the WYFFOS collimator. As WYFFOS is a very suitable instrument, overheads are minimal. More details on the instrument are found in Arribas et al. (1998a, b).

## First Results

INTEGRAL is being used in a number of scientific programs. We give here some examples of recent results obtained with INTEGRAL in different research areas:

- Gravitational lenses (Mediavilla et al., 1998) (Figure 3).
- Detection of faint companions (Arribas et al., 1998b) (Figure 4).
- The study of the circumnuclear region of ultraluminous infrared galaxies (Colina et al., 1999) (Figure 5).
- Structure and dynamics of blue compact dwarf galaxies (García-Lorenzo et al., 2000) (Figure 6).
- The study of the circumnuclear region of active galaxies (García-Lorenzo et al., 1999) (Figure 7).
- The inner regions of M31 (del Burgo et al., 2000).

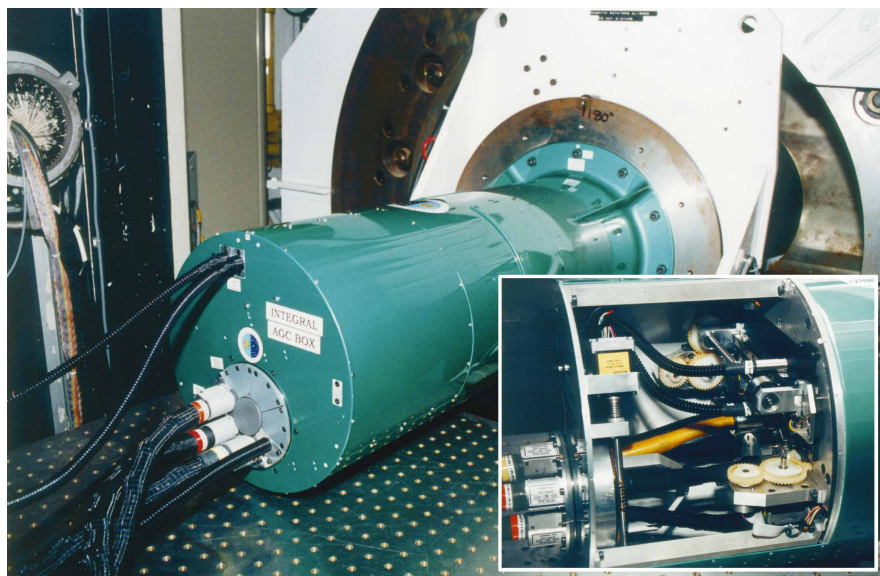


Figure 1. Acquisition, calibration and guiding structure of INTEGRAL.

- X-ray sources in the core of globular clusters (Charles et al., 2000).
- The kinematics of shells in galaxies (Balcells et al., 2000).

What we show here is just a sample of a larger list of projects using INTEGRAL.

### References:

- Arribas, S., Mediavilla, E., Fuensalida, J. J., 1998b, *ApJL*, **505**, 43.  
 Arribas, S., et al., 1998a, *SPIE Proc.*, **3355**, 821.  
 Arribas, S., et al., 1991, *ApJ*, **369**, 260.  
 Balcells, M. et al., 2000, *ApJ*, in press.  
 Bingham, R. G., Gellatly, D. W., Jenkins, C. R., & Worswick, S. P., 1994, *SPIE Proc.*, **2198**, 56.  
 Charles, P. A. et al., 2000, in preparation.

- Colina, L., Arribas, S., & Borne, K. D., 1999, *ApJ*, **527**, L13.  
 del Burgo, C., Mediavilla, E., & Arribas, S., 2000, *ApJ*, in press.  
 García, A., Rasilla, J. L., Arribas, S., & Mediavilla, E., 1994, *SPIE Proc.*, **2198**, 75.  
 García-Lorenzo, B., Arribas, S., & Mediavilla, M., 2000, in Proceedings of "Imaging the Universe in Three Dimensions: Astrophysics With Advanced Multi-Wavelength Imaging Devices", in *ASP Conf. Series*, **195**, 325.  
 García-Lorenzo, B., Cairós, L. M., Caon, N., & Vílchez, J., 2000, in Proceedings of "The Evolution of Galaxies I. Observational Clues", to be published in *ASP Conf. Series*.  
 Mediavilla et al., 1998, *ApJL*, **503**, 27.  
 de Zeeuw, P. T. et al., 2000, *ING Newsletter*, **2**, 11. ☐

Begoña García (bgarcia@ing.iac.es)

	1200 g/mm	600 g/mm	316 g/mm	300 g/mm	Echelle (order 5)
Resolution STD1 (Å)	2.8	6.0	11.8	11	–
Resolution STD2 (Å)	2.8	6.0	11.8	12	–
Resolution STD3 (Å)	4.8	9.8	19.4	12	1.22
Linear dispersion (Å/pix)	1.4	3.1	5.9	19.6	0.35
Spectral coverage (Å)	1445	3140	5837	6144	358

Table 1. Performance of INTEGRAL+WYFFOS combining each fibre bundle with different gratings.

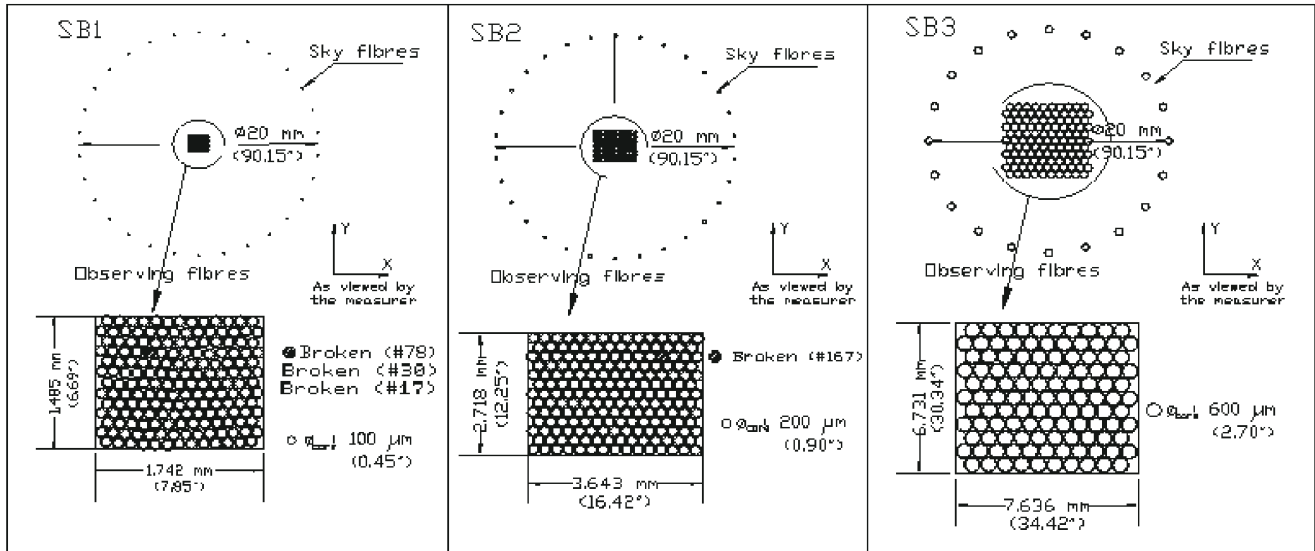


Figure 2. Configuration of the three standard bundles of INTEGRAL at the focal plane of the telescope. Note that the external ring of fibers is intended to collect the sky background simultaneously to the object observations.

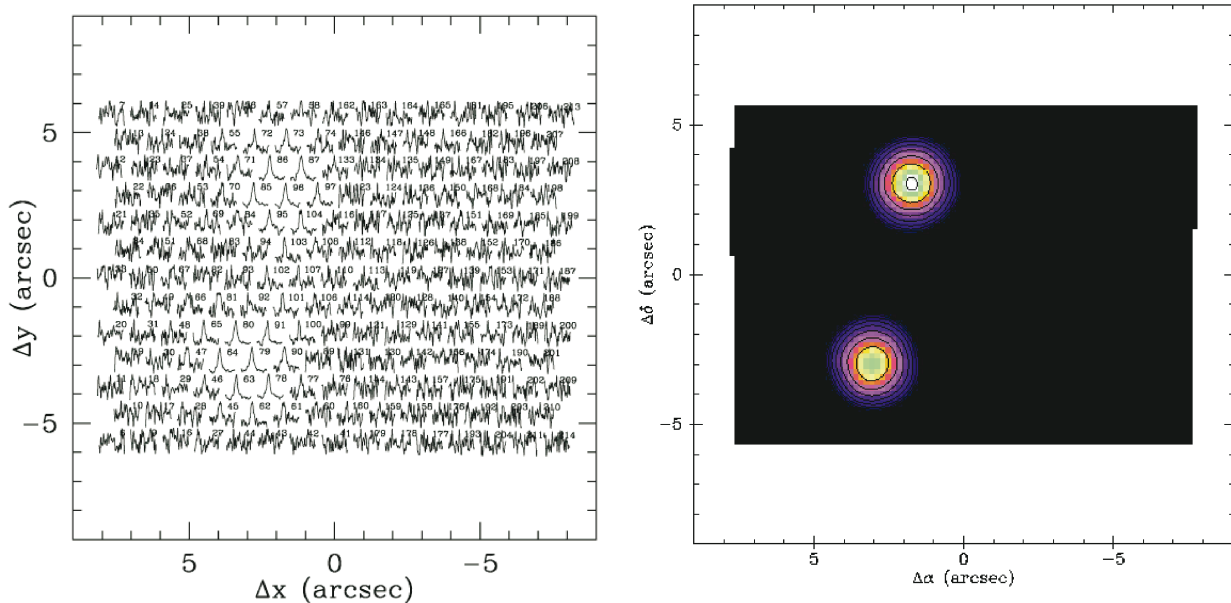


Figure 3. Gravitational lens system Q 0957+561 as observed with INTEGRAL. The picture on the left corresponds to the two-dimensional distribution of the 205 spectra obtained simultaneously with INTEGRAL in the 4500–4700 Å wavelength range (the observed range is much larger). The continuum map (right) is done integrating the flux of the spectra in the 4500–4700 Å wavelength range. The two point-like sources corresponding to the QSO compact images appear well resolved with a separation of 6.17 arcsec, in very good agreement with the distance inferred from the HST images (6.17 arcsec) (courtesy of Veronica Motta).

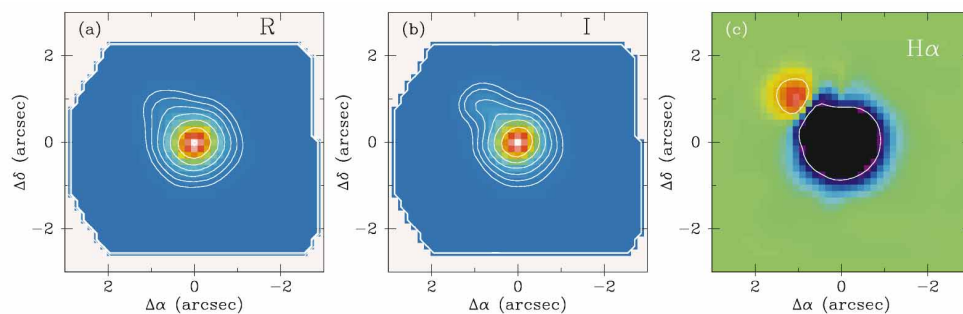


Figure 4. Reconstructed images from INTEGRAL spectra (in R, I, and H $\alpha$ ) of the binary system HD 167605 A+B. This system is formed by two close ( $\sim 1''$ ) stars of about 5 magnitudes of difference in flux. Due to their different spectral type it is possible to select a posteriori a 'filter' to increase the contrast between both objects. These results were obtained with a new technique, Equalized Integral Field Spectroscopy, as explained in Arribas et al. (1998b).



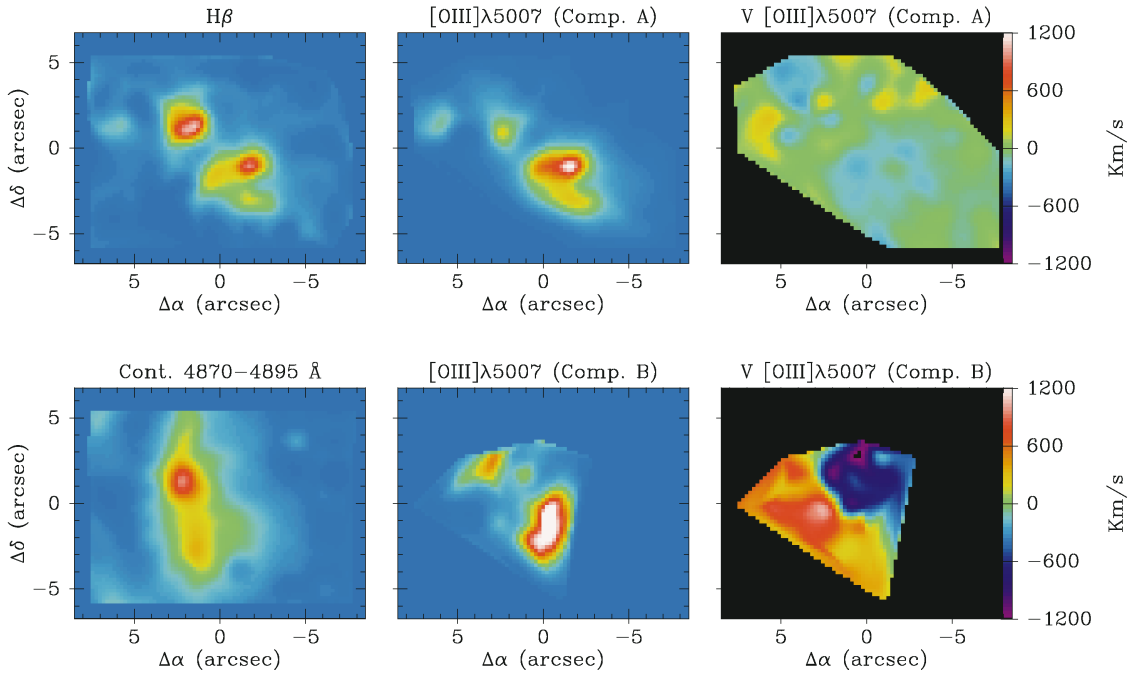


Figure 5. Images of several spectral features and ionised gas velocity fields generated from the *INTEGRAL* spectra of the ultraluminous infrared galaxy Mrk 273. Note the different morphology between the  $H\beta$  and the continuum. The two kinematically distinct components (A and B) could be well separated (by gaussian fits), being their associated velocity fields very different. While one component (A) is rather calm, the other indicates the presence of a strong outflow (more details in Colina et al., 1999).

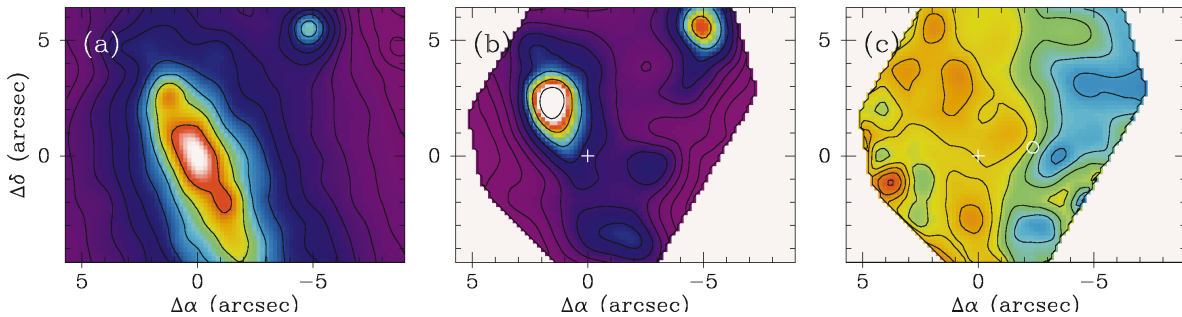


Figure 6. The inner region of the blue compact galaxy Mrk 370 shown by *INTEGRAL*. (a) Reconstructed continuum in the spectral range of the V filter passband; (b)  $[OIII]\lambda 5007$  intensity map; (c) Velocity field of the ionised gas inferred from different emission lines. A white cross marks the optical nucleus. The kinematic centre is indicated by a white circle.

Figure 7. *INTEGRAL* observations of the Seyfert galaxy NGC 2992.

(a) Reconstructed continuum map; (b) Integrated line intensity map of  $[OIII]\lambda 5007$ ; (c) Stellar velocity field inferred from MgI b lines; (d) Velocity field of the ionised gas inferred from cross-correlation in the range 4940–5100 Å, including the  $[OIII]\lambda\lambda 4959, 5007$  emission lines. Isovelocity lines expand from 2100 to 2500 km/s with steps of 20 km/s in both velocity maps. The black cross marks the optical nucleus position.

